

Comparison of Single Heterostructure and Double Heterostructure GaAs-GaAlAs LEDs for Optical Data Links

By A. K. CHIN, G. W. BERKSTRESSER, and V. G. KERAMIDAS

(Manuscript received February 22, 1979)

This paper presents a theoretical and experimental comparison of the performance of single heterostructure (SH) and double heterostructure (DH) GaAs-GaAlAs light-emitting diodes (LEDs). These LEDs are designed for optical data links operating at rates up to T3 (45 Mb/s). The SH LEDs were optimized with respect to active layer carrier concentration and thickness; similar DH LED active layer parameters have not yet been optimized. We find experimentally that the DH diodes launch approximately 8 times the SH power into a butt-coupled, 0.36 numerical aperture (NA), graded-index fiber. Using a diffusion model, we show that the power output of the SH LED is limited by surface recombination and reduced current crowding. These results demonstrate that DH LEDs are necessary for applications requiring high launched power.

I. INTRODUCTION

Burrus-type,¹ single heterostructure (SH) light-emitting diodes (LEDs) are presently fabricated in our laboratory for use in optical data links. Their performance requirements are 45 MHz bandwidth and a minimum butt-coupled power of 10 μ W into a 0.36 numerical aperture (NA), 55- μ m core, graded-index optical fiber at 60 mA forward current. SH LEDs were chosen for the simple growth procedure² and exceptional reliability.³ After optimization of the active layer width and carrier concentration for maximum efficiency while maintaining the required bandwidth, the SH LEDs butt-couple 10 to 15 μ W of power into the fiber. However, initially fabricated, unoptimized double heterostructure (DH) LEDs were found to couple 7 to 8 times more power than the optimized SH LEDs. The purpose of this paper is to explain the difference between the SH and DH LED performance. We begin with an

explanation of the factors influencing the efficiency and bandwidth of the two structures.

Figure 1 is a schematic of our Burrus-type SH and DH LEDs. These LEDs use current crowding by contact area restriction to increase current density for increased brightness. In addition, the localized emission region couples the light more efficiently into the fiber. The contact diameter for both structures is chosen to be $50\text{ }\mu\text{m}$, slightly smaller than the fiber core, for our performance comparison.

Figure 1a shows the design of our SH LED. The active layer is confined on one side by the n-GaAlAs/p-GaAs heterojunction and on the other side by the p-ohmic contact. Since the injected carrier concentration is zero at the p-contact, the p-n junction (i.e., the minority carrier injection source) should be kept at least a minority carrier diffusion length from the contact to minimize nonradiative recombination. However, as the p-n junction is removed in distance from the p-contact, current crowding decreases. Thus, for the SH LED, the active layer width is a compromise between the effects of current crowding and nonradiative recombination at the contact. Five microm-

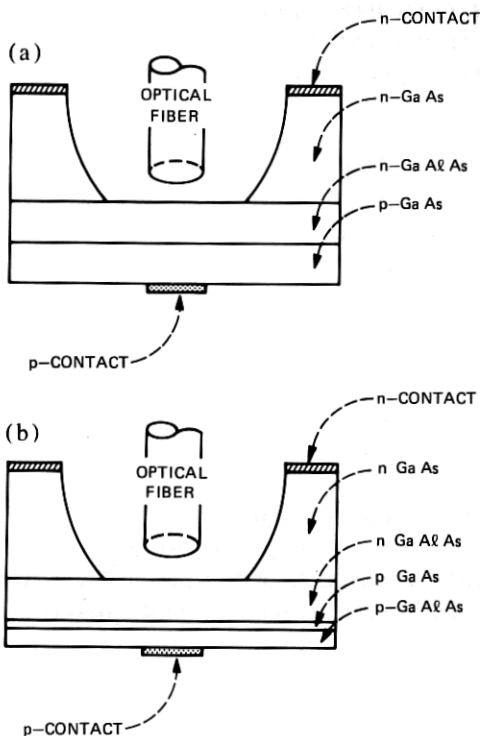


Fig. 1—(a) Schematic of Burrus-type SH LED. (b) Schematic of Burrus-type DH LED.

eters, roughly the electron diffusion length in the p-active layer, is found experimentally to be the optimum active layer thickness.

For the SH LED, the fundamental bandwidth is set by the active layer minority carrier lifetime which depends strongly on the doping density.⁴ For increased doping density, the minority carrier lifetime decreases (i.e., bandwidth increases), but the internal quantum efficiency of the LED also decreases.⁴ To optimize the SH LED performance, the active layer doping density may be chosen so that the minority carrier lifetime is longer than the value necessary to meet the bandwidth requirement. Nonradiative recombination at the p-contact, a result of the compromise in active layer thickness, increases the bandwidth to the required value.

Applying analysis similar to those used for the SH LED, the DH LED is found to be more efficient for the following reasons. First, as seen in Fig. 1b, the active layer of the DH LED is bounded by heterojunctions which have low interface recombination velocities. Second, very thin active and p-GaAlAs carrier confinement layers can be grown so as not to decrease current crowding. For the thickness of $0.7\text{ }\mu\text{m}$ for the active layer and $2\text{ }\mu\text{m}$ for the p-GaAlAs layer, the improved current crowding and carrier confinement of the DH LED results roughly in a factor of 2.5 superior performance compared to the SH LED. Next, when the injected carrier density exceeds the active region doping density, the radiative recombination rate increases with the current density.⁵ This condition, referred to as conductivity modulation or bimolecular recombination, can easily occur only in the DH LED with adequate carrier confinement. As a result, the DH active layer doping density can be chosen at a value well below that necessary to meet the speed requirement to take advantage of the higher internal efficiency; conductivity modulation is used to obtain the higher bandwidth. At the lower doping density ($1 \times 10^{17}\text{ cm}^{-3}$), the DH LED has twice the internal quantum efficiency of the higher doped ($1 \times 10^{19}\text{ cm}^{-3}$) SH LED.⁴ Our analysis thus accounts for a total factor of 5 between the performance of the SH and DH LEDs.

Detailed discussion of the above points is contained in the subsequent sections.

II. MATERIAL-RELATED PARAMETERS

In this section, we discuss the selection of active layer hole concentration for $\sim 70\text{-MHz}$ bandwidth SH and DH LEDs and the effect of the hole concentration on the internal efficiency of the LEDs.

2.1 Lifetime

For T3 data rate (45-Mb/s) optical communication systems, the LED should have an approximate 70-MHz bandwidth (pulse decay time $\tau \approx$

2.3 ns).^{*} The higher speed is needed to allow for receiver response time and dispersion in the optical fiber.⁶ To obtain this large bandwidth, the active layer must be chosen with a minority carrier lifetime equivalent to the required bandwidth, or the device structure must be appropriately designed to increase the speed. For a SH LED, the device time constant can only be reduced by nonradiative recombination, e.g., surface recombination. On the other hand, nonradiative recombination or bimolecular recombination (conductivity modulation) may be used to increase the bandwidth of a DH LED. This mechanism also minimizes the loss due to interface recombination by reducing the diffusion length.

Figure 2 shows the decay time of DH LEDs as a function of active layer hole concentration. This figure is taken from Nelson.⁴ The decay times shown are essentially structure-independent, since the effects of surface recombination and conductivity modulation were minimized. These values are somewhat larger than the minority carrier lifetime because of the effects of photon recycling, but they can be considered to be minimum bulk lifetimes.⁴

From Fig. 2, the active layer hole concentration of SH LEDs should be chosen in the range $p \approx 8 \times 10^{18} \text{ cm}^{-3}$ to have a 70-MHz bandwidth. Due to the trade-offs between current crowding and surface recombination, the range $p \approx 6 \times 10^{18} \text{ cm}^{-3}$ is allowable. In optimizing the active layer width, an increase in bandwidth and a reduction in efficiency due to surface recombination is also obtained. For 70-MHz DH LEDs, a lower active layer hole concentration range ($p \approx 10^{17} \text{ cm}^{-3}$) can be used. A hole concentration below 10^{18} cm^{-3} is desirable for increasing the internal efficiency, while bimolecular recombination which maintains bulk efficiency is used to decrease the decay times from the values shown in Fig. 2.

2.2 Internal efficiency

Figure 3 shows the bulk efficiency of p-GaAs decreasing rapidly for $p > 10^{18} \text{ cm}^{-3}$ at both high and low carrier injection. This figure is also taken from Nelson,⁴ and the details of obtaining the data may be found there. For both low and high electron injection, the bulk efficiency at $p = 1 \times 10^{17} \text{ cm}^{-3}$ is approximately twice that at $p = 1 \times 10^{19} \text{ cm}^{-3}$. The decrease in bulk efficiency at high doping density is presumably due to the introduction of nonradiative recombination centers.⁴ Thus, since the active layer of SH LEDs must be doped approximately 10^{19} cm^{-3} to obtain a 70-MHz bandwidth while only 10^{17}

^{*} The pulse decay time (τ) is the time for the LED light output to decay to $1/e$ of its peak value. τ is related to the 90-percent to 10-percent fall time $\tau_{90\%-10\%}$ by the relation: $\tau_{90\%-10\%} = 2.2\tau$.

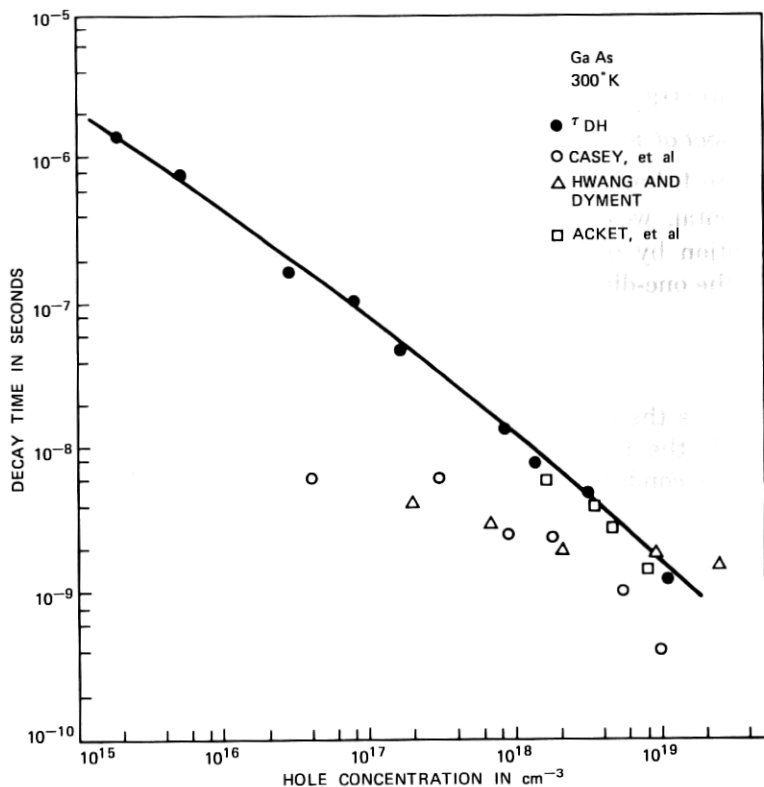


Fig. 2—Variation of photo-luminescent decay times with doping level (from Ref. 4).

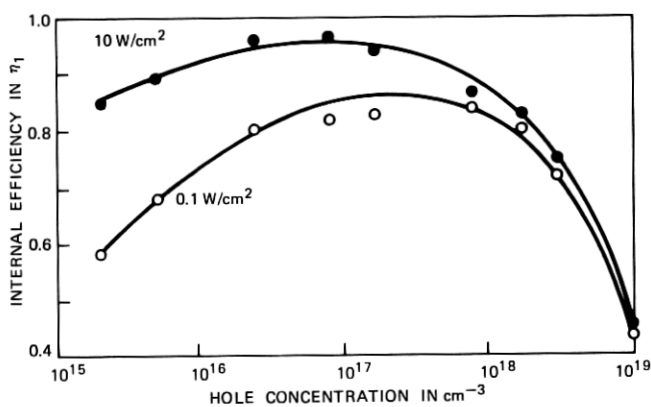


Fig. 3—Variation of internal quantum efficiency with doping level at two different excitation rates (from Ref. 4).

cm^{-3} hole concentration is required for DH LEDs, the DH LED should have twice the efficiency of the SH LED.

III. STRUCTURAL PARAMETERS

3.1 Effect of surface recombination and self absorption

Figure 4 shows a DH structure and two SH structures. Following Lee and Dentai,⁷ we estimate the effects of surface recombination and self-absorption by using a one-dimensional diffusion model. At steady state, the one-dimensional continuity equation is given by

$$D \frac{d^2 n}{dx^2} - \frac{n}{\tau} = 0, \quad (1)$$

where n is the excess electron density, D is the electron diffusivity, and τ is the bulk electron lifetime.⁷ As shown in the figure, the boundary conditions for each of the three structures are

DH

$$-\left. \frac{dn}{dx} \right|_{x=0} = \frac{J}{eD} - \frac{s}{D} n(o) \quad (2)$$

$$-\left. \frac{dn}{dx} \right|_{x=w} = \frac{s}{D} n(w) \quad (3)$$

SH₁

$$-\left. \frac{dn}{dx} \right|_{s=0} = \frac{J}{eD} \quad (4)$$

$$-\left. \frac{dn}{dx} \right|_{x=w} = \frac{s}{D} n(w) \quad (5)$$

SH₂

$$-\left. \frac{dn}{dx} \right|_{x=0} = \frac{J}{eD} - \frac{s}{D} n(o) \quad (6)$$

$$n(w) = 0, \quad (7)$$

where w is the active layer width, s is the interfacial recombination velocity at the heterojunction interfaces, and J is the current density at the p-n junction. Table I lists $n(x)$, the solution to the diffusion equation, for the three structures. Taking into account self-absorption in the active region, the light intensity (P) from the p-n junction side of the LED is given by

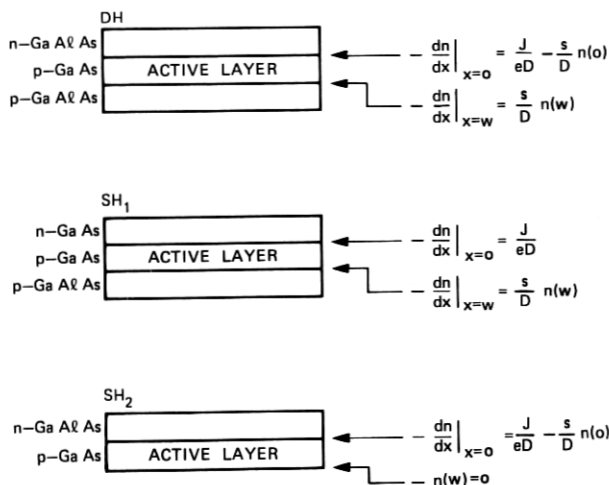


Fig. 4—Boundary conditions for a DH LED and two SH LEDs.

Table I

	DH, SH ₁	SH ₂
$n(x)$	$\frac{JL}{eD} \left\{ \frac{\cosh\left(\frac{w-x}{L}\right) + S \sinh\left(\frac{w-x}{L}\right)}{DEN} \right\}$	$\frac{JL}{eD} \frac{\sinh\left(\frac{w-x}{L}\right)}{DEN}$
$\frac{\tau_{eff}}{\tau}$	$\frac{\sinh\left(\frac{w}{L}\right) + S \left[\cosh\left(\frac{w}{L}\right) - 1 \right]}{DEN}$	$\frac{\cosh\left(\frac{w}{L}\right) - 1}{DEN}$
η_s	$\frac{1}{2 DEN} \left\{ \frac{1+S}{1+\alpha L} \left[1 - e^{\frac{-w}{L}(1+\alpha L)} \right] e^{\frac{w}{L}} - \frac{1-S}{1+\alpha L} \left[1 - e^{\frac{w}{L}(1-\alpha L)} \right] e^{\frac{-w}{L}} \right\}$	$\frac{1}{2 DEN} \left\{ \frac{1}{1+\alpha L} \left[1 - e^{\frac{-w}{L}(1+\alpha L)} \right] e^{\frac{w}{L}} - \frac{1}{1-\alpha L} \left[1 - e^{\frac{w}{L}(1-\alpha L)} \right] e^{\frac{-w}{L}} \right\}$

$$S = \frac{Ls}{D}$$

$$DEN_{DH} = (S^2 + 1) \sinh\left(\frac{W}{L}\right) + 2S \cosh\left(\frac{W}{L}\right)$$

$$DEN_{SH_1} = \sinh\left(\frac{W}{L}\right) + S \cosh\left(\frac{W}{L}\right)$$

$$DEN_{SH_2} = \cosh\left(\frac{W}{L}\right) + S \sinh\left(\frac{W}{L}\right)$$

$$P = \frac{1}{2} \frac{h\nu}{\tau_r} \left\{ \int_0^w n(x) e^{-\alpha x} dx + R e^{-2w\alpha} \int_0^w n(x) e^{\alpha x} dx \right\}. \quad (8)$$

The second term in the equation is the reflected power from the contact. Absorption losses due to the additional layer for the DH and SH₁ case are neglected. The emission frequency is ν , the contact reflectivity is R , the radiative lifetime is τ_r , and the absorption coefficient is α . The external efficiency of the LED is defined by

$$\eta_s = \frac{P}{J} \left(\frac{e}{h\nu} \right) \frac{\tau_r}{\tau}. \quad (9)$$

Table I also lists η_s for the three structures.

Comparing the solutions for SH₁ and DH diodes, only a small difference is noted for $sL/D \ll 1$. In the range of thickness to which these equations are applied, the discussions concerning interface recombination and self-absorption for the DH device refer also to the SH₁ device. The one disadvantage of the SH₁ structure relative to the DH structure is the lack of carrier confinement at the homojunction. Thus SH₁ is equivalent to DH under conditions where conductivity modulation is not important, but becomes less efficient at high carrier injection. The SH LED discussed in the following sections refers only to SH₂.

Figure 5a displays the calculated SH external efficiency as a function of the active layer width for several diffusion lengths; Fig. 5b shows similar curves for the DH case. The calculation parameters are listed on the figures. Values for $1 \times 10^{17} \text{ cm}^{-3}$ and $1 \times 10^{19} \text{ cm}^{-3}$ p-doping are chosen for the DH and SH case, respectively, for comparison with fabricated devices.

The fabricated SH LEDs are analyzed using the 5- μm SH efficiency curve in Fig. 5a, since a 5- μm minority carrier diffusion length was measured on 10^{19} cm^{-3} p-type GaAs using electron-beam-induced current (EBIC).⁸ A peak in the SH efficiency results from the high p-contact surface recombination for small w and self-absorption for large w . The peak efficiency of 0.48 at $w = 12 \mu\text{m}$ is inconsistent with the experimentally determined optimum layer thickness of 5 μm . Better agreement between calculation and experiment is found when current crowding is considered.

For the DH case, an 11- μm diffusion length is derived from the device decay time of $\sim 3 \text{ ns}$. The high output power of the DH LED with $w = 0.5 \mu\text{m}$ is consistent with the high calculated efficiency shown in Fig. 5b. This consistency is maintained when current crowding is considered.

3.2 Device bandwidths

The effective device lifetime can be obtained from the carrier concentration by averaging over the active region:⁷

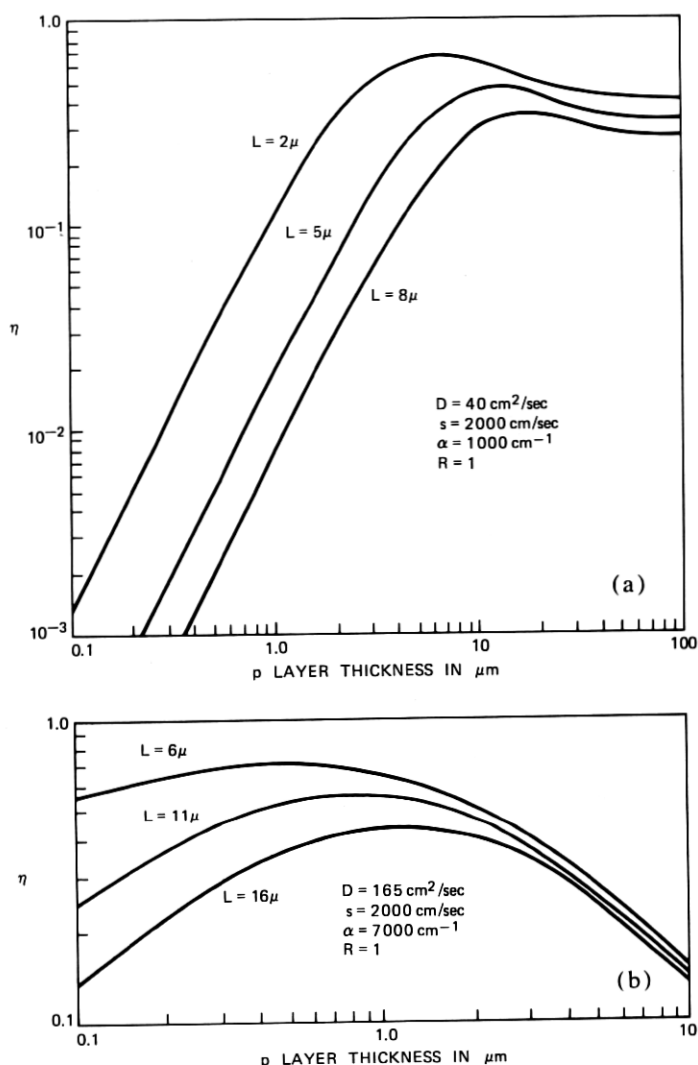


Fig. 5—(a) SH efficiency vs p-layer thickness for indicated electron diffusion lengths. Material parameters are for 10^{19} cm^{-3} doping. (b) DH efficiency vs p-layer thickness for indicated electron diffusion lengths. Material parameters are for 10^{17} cm^{-3} doping.

$$\bar{n} = \frac{1}{w} \int_0^w n(x) dx \equiv \frac{J}{e} \frac{\tau_{eff}}{w}. \quad (10)$$

τ_{eff}/τ is listed in Table I for the three structures of Fig. 3.

Figure 6a plots the calculated values of τ_{eff}/τ as a function of p-layer thickness for the SH₂ LED. The material parameters in the calculation are those of 10^{19} cm^{-3} Ge-doped GaAs for comparison with fabricated SH LEDs. The diffusion length is varied to show the effect of surface

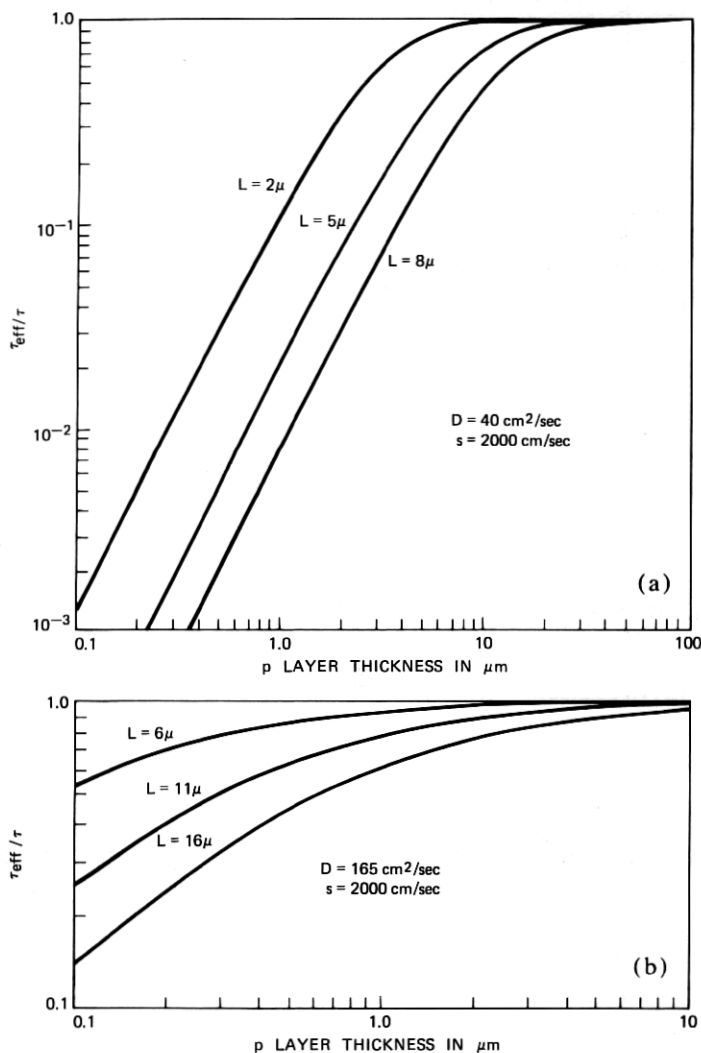


Fig. 6—(a) Normalized SH effective decay time vs p-layer thickness for indicated electron diffusion lengths. Material parameters are for 10^{19} cm^{-3} doping. (b) Normalized DH effective decay time vs p-layer thickness for indicated electron diffusion lengths. Material parameters are for 10^{17} cm^{-3} doping.

recombination. For a $5\text{-}\mu m$ diffusion length and p-layer thickness of $5 \mu m$, surface recombination reduces the decay time by 0.35. Using the 1- to 2-ns decay time for 10^{19} cm^{-3} GaAs from Fig. 2, a device decay time of 0.35 to 0.7 ns is obtained. This value appears to be in disagreement with the measured value of 2.5 ns, but the device lifetime is probably the result of photon recycling in the thick p-layer.⁴

Figure 6b plots the calculated values of τ_{eff}/τ as a function of p-layer thickness for the DH LED. The material parameters of 10^{17} cm^{-3} Ge-doped GaAs are used in the calculation for comparison with fabricated devices. The diffusion length is again varied to show the effect of surface recombination. A diffusion length of $11 \mu\text{m}$ is obtained from the bimolecular recombination time constant of 7.3 ns and a diffusivity of $165 \text{ cm}^2/\text{s}$.⁹ The bimolecular recombination time for our DH LEDs is given by⁷

$$\tau_{BR} = B \left(\frac{J}{ewB} \right)^{-1/2}, \quad (11)$$

where $B = 5 \times 10^{-11} \text{ cm}^3/\text{s}$ is the recombination probability, $w = 0.5 \mu\text{m}$ is the active layer width, and $J = 3000 \text{ A/cm}^2$ is the current density. τ_{BR} is used in the analysis rather than the decay time in Fig. 1, since the injected carrier density

$$\Delta n = \left(\frac{J}{ewB} \right)^{1/2} = 2.8 \times 10^{18} \text{ cm}^{-3} \quad (12)$$

is an order of magnitude greater than the doping concentration. From Fig. 6b, at $0.5\text{-}\mu\text{m}$ active layer width, τ_{BR} is reduced by a factor of 0.63 due to interface recombination to give a device decay time of $\sim 4.5 \text{ ns}$. This value is consistent with the $\sim 3.5\text{-ns}$ decay time measured on DH LEDs at 60 mA ($J = 3000 \text{ A/cm}^2$) forward bias.

3.3 Current crowding

The simplest method of coupling a LED to an optical fiber is to butt the fiber end directly to the LED. To maximize this coupling, the light-emitting area should be limited to the fiber core size. The graded-index fiber used for the present study has a $55\text{-}\mu\text{m}$ diameter core. The SH and DH LEDs were fabricated with a $50\text{-}\mu\text{m}$ contact to localize the light-emitting area.

The SH and DH LEDs are Burrus-type diodes where a well has been opened in the opaque n-GaAs substrate to access the generated light. The current is confined to flow through the $50\text{-}\mu\text{m}$ contact by a SiN_x insulating coating. The current density and distribution in the active region is determined by the active layer width and the sheet resistivity of the active layer. A thicker layer width or lower sheet resistivity results in a lower current density above the contact and a larger emitting area. This current spreading reduces the coupling efficiency and, in the DH case, the bimolecular recombination. An improvement may be made by reducing the contact dimension, but a lower limit of $25 \mu\text{m}$ is set by the use of an evaporation mask to define the contacts.

Using the technique described by Joyce and Wemple,¹⁰ the calcu-

lated current density (J) at the p-n junction above the contact is plotted as a function of p-layer thickness in Fig. 7. The calculation parameters are indicated on the figure. The current density is a strong function of the p-layer thickness; the current density is half the maximum value of 2500 A/cm^2 by $w \sim 1.5 \mu\text{m}$. The other two curves in the figure are the product of the current density times the calculated external efficiency ($\eta \times J$) of the SH and DH LEDs. The effect of the bottom confinement layer for the DH structure is neglected in the current density calculation, since the figure is meant to show only the approximate behavior with thickness.

The calculation of the SH efficiency uses the 10^{19} cm^{-3} Ge-doped GaAs parameters (listed on the figure) for comparison with fabricated devices. The absorption coefficient and interface recombination velocity are from Ref. 7, and the electron diffusivity is obtained from Ref. 9. The electron diffusion length was measured using the electron beam induced current technique.⁸ As shown in Fig. 7, the $\eta_{\text{SH}} \times J$ curve shows a peak for an active layer width between 2 and $3 \mu\text{m}$. $\eta_{\text{SH}} \times J$ is limited by surface recombination for thin layers and self-absorption or current spreading for thick layers. The calculated optimum active

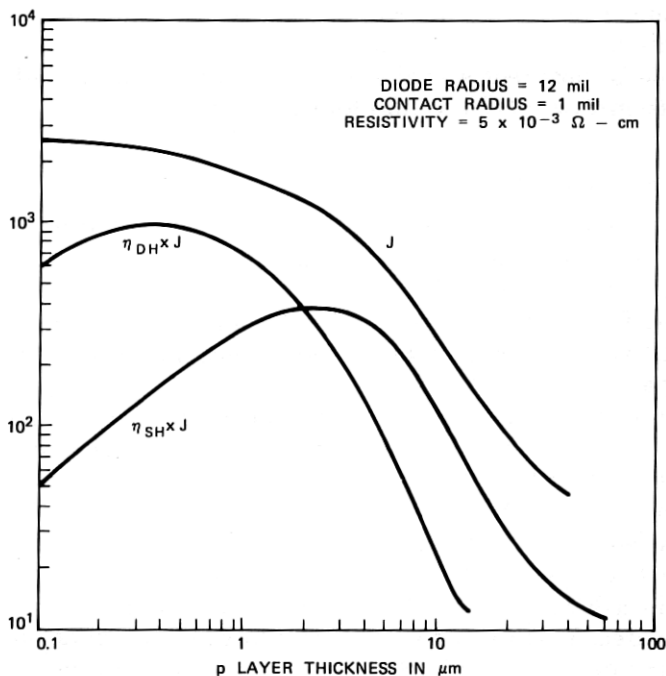


Fig. 7— J , $\eta_{\text{DH}} \times J$, and $\eta_{\text{SH}} \times J$ vs p-layer thickness. J is the current density for the diode parameters indicated at a forward current of 60 mA, η_{DH} is the DH efficiency for an 11- μm diffusion length from Fig. 5b, and η_{SH} is the SH efficiency for a 5- μm diffusion length from Fig. 5a.

layer thickness is lower than the experimentally determined value of $\sim 5 \mu\text{m}$ for SH LEDs. However, small variations in the many variables that went into the calculation may easily shift the optimum value to $\sim 5 \mu\text{m}$.

In the $\eta_{\text{DH}} \times J$ calculation, the optimum active layer thickness is determined to be between 0.2 and 0.7 μm . The material parameters corresponding to 10^{17} cm^{-3} Ge doping were used. The diffusion length was corrected for the effects of bimolecular recombination. A peak occurs in $\eta_{\text{DH}} \times J$ for the reasons given in the SH case. The 0.5- μm active layer width of the fabricated DH LEDs lies within the calculated optimum range. From Fig. 7, $\eta_{\text{DH}} \times J$ for $w = 0.5 \mu\text{m}$ is approximately 2-1/2 times the peak value of $\eta_{\text{SH}} \times J$.

IV. SUMMARY

We have compared SH and DH LEDs designed for optical communications at T3 data rate. Our analysis shows a factor-of-2 loss in the internal efficiency of the SH LED due to the introduction of nonradiative recombination centers at the high active layer doping level required by the SH devices. An additional factor-of-2.5 loss was found in the external efficiency of the SH LED, resulting from surface recombination at the p-contact and the self absorption and current spreading in the thicker active layer of the SH LED. The total factor-of-5 difference between SH and DH LEDs based on the arguments in this paper is in reasonable agreement with the experimentally determined value of 7 to 8, since the calculations involved many variables. These results demonstrate that DH LEDs are required for data links limited by power launched into the optical fiber.

V. ACKNOWLEDGMENTS

One author (AKC) is indebted to O. G. Lorimor and R. J. Nelson for many discussions on diode parameters. We would also like to acknowledge helpful discussions with R. H. Saul, T. P. Lee, H. J. Leamy, W. H. Hackett, F. R. Nash, and S. E. Haszko.

REFERENCES

1. C. A. Burrus and B. I. Miller, *Opt. Commun.*, **4** (1971), p. 307.
2. V. G. Keramidas, G. W. Berkstresser, and C. L. Zipfel, unpublished work.
3. C. L. Zipfel, R. H. Saul, and V. G. Keramidas, paper presented at DRC, Boulder, Colorado (1979).
4. R. J. Nelson and R. G. Sobers, *J. Appl. Phys.*, **49** (1978), p. 6103.
5. H. Namizaki, H. Kay, M. Ishii, and A. Ito, *Appl. Phys. Lett.*, **24** (1974), p. 486.
6. H. Temkin, private communication.
7. T. P. Lee and A. G. Dentai, *IEEE J. Quantum Elec.*, **14** (1978), p. 150.
8. A. K. Chin, unpublished work.
9. M. Ettenberg, H. Kressel, and S. L. Gilbert, *J. Appl. Phys.*, **44** (1973), p. 827.
10. W. B. Joyce and S. H. Wemple, *J. Appl. Phys.*, **41** (1970), p. 3818.